A surface chemistry model for nonreactive trace gas adsorption on ice: Implications for nitric acid scavenging by cirrus

A. Tabazadeh[1], O. B. Toon[2], and E. J. Jensen[1]

Abstract. According to recent measurements HNO_3 nearly saturates laboratory ice films in flow tubes for vapor pressures above 10^{-7} torr and temperatures below 230 K. In the upper troposphere the HNO_3 vapor pressure is in the range of 1 to 3 $\times 10^{-8}$ torr and therefore the current laboratory estimates of saturation may not hold in the atmosphere. Here, with the aid of a surface chemistry model and laboratory data we estimate that the binding energy for HNO_3 adsorbed on ice is about -14.2 ± 0.2 kcal mol^{-1}. Using the surface model, we explore the sensitivity of HNO_3 scavenging efficiency to cirrus cloud temperature, ice number density, and HCl competitive co-adsorption.

Introduction

Ozone production in the upper troposphere is catalyzed primarily by nitrogen oxides [*Singh et al.*, 1996; *Jacob et al.*, 1996]. Since ozone is an effective greenhouse gas in the upper troposphere [*Lacis*, 1990], it is important to understand the distribution of nitrogen between nitrogen oxides and their main reservoir species, HNO_3. Overall, global transport-chemistry models overestimate the abundance of gas phase HNO_3 in the upper troposphere compared to observations [*Thakur et al.*, 1999], particularly during spring and summer [*Tabazadeh et al.*, 1998]. It has been suggested that cirrus clouds provide an important global sink for HNO_3 in the upper troposphere [*Lawrence and Crutzen*, 1998]. Here, by using a surface chemistry model, we investigate under what set of conditions and assumptions cirrus can be considered as an important potential scavenger of HNO_3 in the upper troposphere.

Surface Chemistry Model Description

The Langmuir surface chemistry model used here is described in detail by *Tabazadeh and Turco* [1993] with one major modification. In the analysis described here we assume a dissociated rather than a molecular state for HNO_3 and/or HCl adsorbed on ice in agreement with laboratory studies, indicating that both HCl and HNO_3 ionize on ice surfaces [*Abbatt et al.*, 1992; *Zondlo et al.*, 1997]. For clarity of presentation the preexponential factors for the adsorption and desorption rate constants are simplified compared to the relations given in *Tabazadeh and Turco* [1993] .

The rate of gas adsorption onto a solid surface for a mobile film is given by [*Laidler et al.*, 1940],

[1]NASA Ames Research Center, Moffett Field, CA
[2]Laboratory for Atmospheric and Space Physics, University of Colorado, Boulder, CO

$$k_a = \frac{C}{\sqrt{MT}} \exp\left\{ \frac{-e_1}{RT} \right\} \qquad (1)$$

where $C = 1.111 \times 10^6$ $(kg^{1/2}K^{1/2}torr^{-1}sec^{-1})$, M is molecular weight of the adsorbing gas in kg, T is temperature in K, R is the gas constant, and e_1 is the energy of activation for adsorption per single molecule.

The rate of gas desorption is given by [*Laidler et al.*, 1940],

$$k_d = 10^{13}(sec^{-1}) \exp\left\{ \frac{-e_2}{RT} \right\} \qquad (2)$$

where e_2 represents the energy of activation for the desorption of a single molecule. The equilibrium adsorption constant K_{eq} is defined as

$$K_{eq} = \frac{k_a}{k_d} = \frac{C}{10^{13}(sec^{-1)} \sqrt{MT}} \exp\left[\frac{\Delta G_{ads}}{RT} \right] \qquad (3)$$

where $\Delta G_{ads} = -(e_2 - e_1)$ is the free energy of adsorption per single molecule. Here we assume that ΔG_{ads} is independent of temperature.

Assuming that HNO_3 dissociates on the ice surface, the adsorption process can be presented by the following chemical equation:

$$HA(gas) \overset{K_{eq}}{\Longleftrightarrow} H^+(ad) + A^-(ad) \qquad (4)$$

In the case of a nonreactive dissociative gas, the Langmuir isotherm describes the interaction of the gas with the surface in terms of the equilibrium surface coverage (θ), given by

$$\theta = \frac{\alpha K_{eq}^{1/2} P_g^{1/2}}{1 + K_{eq}^{1/2} P_g^{1/2}} \qquad (5)$$

where P_g is the vapor pressure of the adsorbed gas over the surface in units of torr, and α is the fraction of surface sites that are available for adsorption.
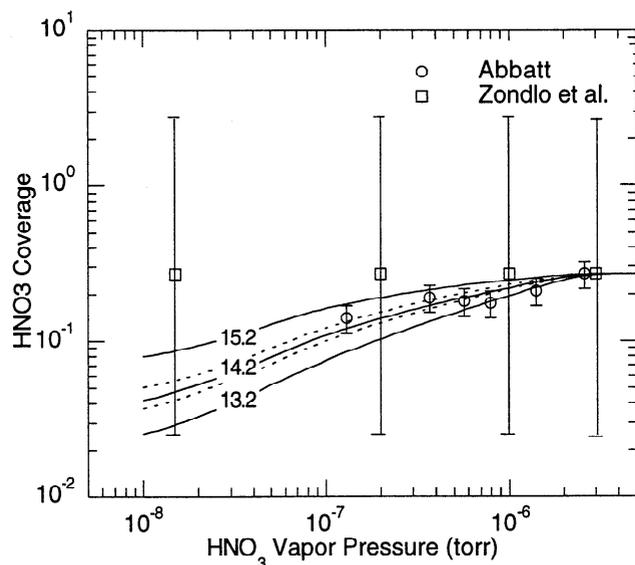
Overall for most surface chemistry studies the adsorbing material is nonvolatile (i.e., H_2 adsorption on the silicon surface). Thus all the surface sites are initially available for adsorption. However in the upper troposphere the most likely adsorbing surface is ice, which is volatile and therefore some of the surface sites on ice are occupied by H_2O molecules that continuously adsorb and desorb from the surface. Since the remaining vapor pressure of H_2O over ice greatly exceeds the mixing ratios of trace gas species, such as HNO_3 and HCl, a significant fraction of surface sites on ice are taken up by water and their effect on the adsorption process in the atmosphere must be accounted for.

Laboratory Data Interpretation and Analysis

Figure 1 illustrates the variation of HNO_3 coverage on ice as a function of vapor pressure for different assumptions of ΔG_{ads} calculated using equations (1) through (6). Also plotted are raw laboratory adsorption data [*Abbatt*, 1997; *Zondlo et al.*, 1997]. Using $\Delta G_{ads} = -14.2 \pm 0.2$ kcal mol^{-1} in equations (1) through (5) yields a factor of about two change in the coverage in agreement with the laboratory data of Abbatt at 228 K over the vapor pressure range of 1.3×10^{-7} torr to 3.1×10^{-6} torr (see Figure 1). In addition, Abbatt data suggests that the HNO_3 coverage on ice at full saturation is near 2.7×10^{14} molecules cm^{-2} at 228 K, which is equivalent to about 27 % of the total number of sites ($\sim 10^{15}$ cm^{-2}) available for adsorption on a typical surface [*Adamson*, 1989]. Assuming that the HNO_3 coverage on ice at full saturation is 27% at 228 K, the extrapolation of Abbatt's data to lower vapor pressures using the model yields a coverage of about 0.04 monolayer ($\sim 5 \times 10^{13}$ molecules cm^{-2}) of HNO_3 on ice at 10^{-8} torr. Also plotted in Figure 1 is the data of Zondlo et al., which is consistent with an adsorption energy equal or greater than -13.2 kcal mol^{-1} in magnitude. In Figure 2 the sensitivity of HNO_3 surface coverage to temperature is shown for different assumptions of the adsorption free energy. A factor of 4 change in the observed coverage is only consistent with an adsorption energy of -14.2 ± 0.2 kcal mol^{-1}. Thus using an adsorption free energy of -14.2 ± 0.2 kcal mol^{-1} in the model reproduces well

Figure 2. HNO_3 coverage as a function of temperature for different assumptions of the adsorption free energy calculated at a constant HNO_3 vapor pressure of 7.5×10^{-7} torr. The adsorption free energies used in the model are labeled on the lines and are in units of negative kcal mol^{-1}. The dashed lines represent model calculations for adsorption free energies of -14 and -14.4 kcal mol^{-1}. Also plotted are raw laboratory data from *Abbatt* [1997]. The model lines are normalized to a saturation limit of 0.29, the maximum HNO_3 coverage measured by Abbatt.

the observed trends [*Abbatt*, 1997] in both pressure and temperature.

Atmospheric Applications

In the pervious section we emphasized the fact that in order to extrapolate HNO_3 laboratory coverages into atmospherically relevant values, the use of a surface adsorption model is required. In other words, it is incorrect to assume that since laboratory coverages are, for example, a significant fraction of a monolayer, then atmospheric coverages are also the same fraction of a monolayer irrespective of temperature and pressure dependencies. In addition, for computing atmospheric coverages, the surface adsorption model must be coupled to mass conservation relations for all the species adsorbed on the surface. To include the effect of HNO_3 depletion on the coverage, the following equations must be solved simultaneously:

$$P_T = P_g + P_a \qquad (6a)$$

$$\theta = \frac{\alpha K_{eq}^{1/2} P_g^{1/2}}{1 + K_{eq}^{1/2} P_g^{1/2}} \qquad (6b)$$

$$\theta = \frac{\beta Pa}{\sigma S} \qquad (6c)$$

Where P_T is the total HNO_3 partial pressure in torr, P_g is the atmospheric equilibrium HNO_3 vapor pressure over ice in torr, P_a is the HNO_3 concentration in the adsorbed state in torr, β ($= 9.656 \times 10^{18} T^{-1}$) is a conversion factor, σ ($= 10^{15}$) is the surface site density in cm^{-2}, and S is the ice surface area density in cm^2 cm^{-3}. By iterating the above equations P_g can be

Figure 1. HNO_3 coverage on ice as a function of vapor pressure for different assumptions of the adsorption free energy at 228 K. The adsorption free energies are labeled on the chart and are in units of negative kcal mol^{-1}. The dashed lines represent model calculations for adsorption free energies of -14 and -14.4 kcal mol^{-1}. Also plotted are raw laboratory data from *Abbatt* [1997] and *Zondlo et al.* [1997]. Since the porosity of ice films produced using different laboratory techniques are different, the data of Zondlo et al. is normalized to the saturation limit of Abbatt's data (coverage = 0.27) in order to illustrate how the two sets of laboratory measurements compare against each other. The error bars shown are about 15 % and a factor of 10 [Mark Zondlo, Personal Communication, 1999] for the Abbatt and the Zondlo et al. data, respectively. The model lines are normalized to a saturation limit of 0.27, the maximum HNO_3 coverage measured by Abbatt at 228 K.

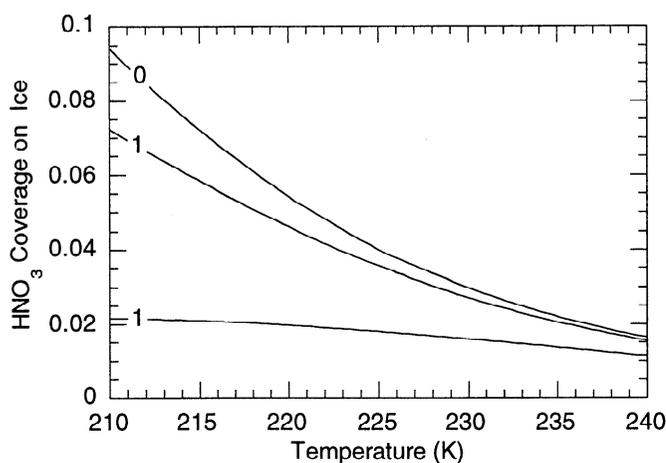evaluated as a function of P_T, temperature, and ice surface area density.

In addition, ice particle surfaces in the atmosphere may differ greatly from pristine surfaces generated in the laboratory. For instance, the adsorption of HCl (or other trace species) on ice may significantly reduce the HNO_3 coverage as a result of competitive adsorption. To account for HCl competition equation (6b) must be replaced by:

$$\theta = \frac{\alpha K_{eq}^{1/2} P_g^{1/2}}{1 + K_{eq}^{1/2} P_g^{1/2} + K_{eq,HCl}^{1/2} P_{g,HCl}^{1/2}} \quad (7)$$
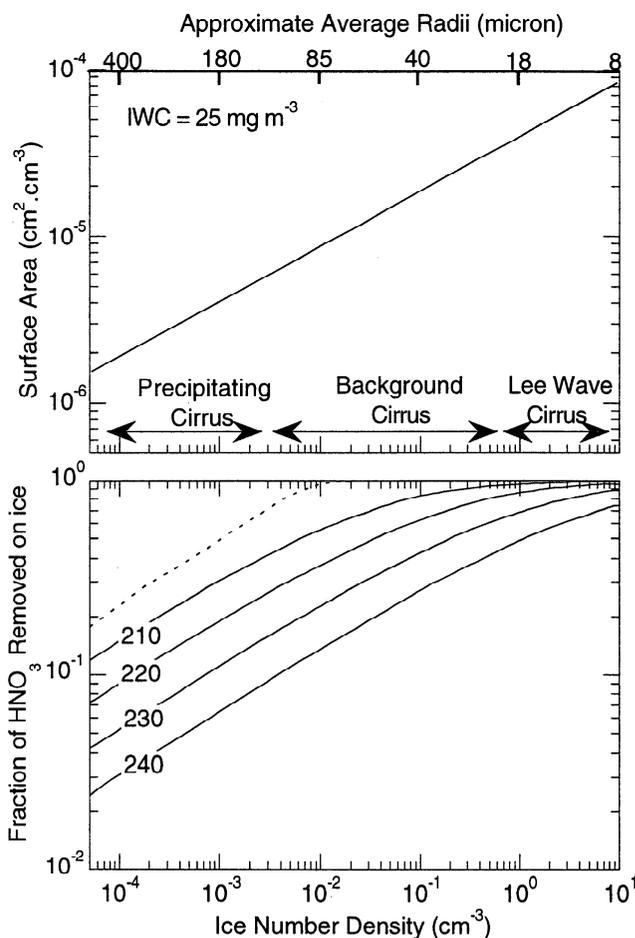
Adding the mass balance relations for HCl uptake on ice to the above set of equations (6a-6c), the effect of HCl in reducing the HNO_3 coverage can be evaluated. As shown in Figure 3, for a typical HNO_3/HCl mole ratio of 2 [Brasseur and Solomon, 1986], HCl can potentially reduce the HNO_3 coverage on cirrus by about 30 % at ~ 210 K if the adsorption energy for HNO_3 and HCl binding on ice are equivalent. On the other hand, if the HCl adsorption energy on ice is larger than that of HNO_3, then the HNO_3 coverage on ice may be reduced by as much as a factor of 4 due to the HCl competitive adsorption (Figure 3).

In Figure 4 the fraction of HNO_3 removed on ice (P_a / P_T) is calculated as a function of temperature using equation (6). A typical global ice water content (IWC) for cirrus inferred from lidar and radar studies is about 25 mg m^{-3} [Dowling and Radke, 1990; Mace et al., 1997]. The surface areas shown in Figure 4 are calculated by distributing 25 mg m^{-3} of water over a monodispersed size distribution of ice crystals with different number densities, which are indicated on top of the chart. It is important to point out that our results shown in Figure 1 don't take into account the effect of HNO_3 taken up in the bulk of ice particles. However new laboratory data suggest that the HNO_3 bulk uptake is negligible and can be ignored [Sommerfeld et al., 1998].

As shown in Figure 4 near complete removal of HNO_3 on cirrus can occur in ice wave clouds, in agreement with in situ

Figure 4. HNO_3 fraction removed on ice as a function of ice number density and temperature calculated for a HNO_3 ambient vapor pressure of 2 x 10^{-8} torr. The model results are calculated using equations (1) through (7) by setting ΔG_{ads}= -14.2 kcal mol^{-1} and α = 0.25. The dotted line labeled as Lawrence and Crutzen [1997] is calculated assuming that the HNO_3 coverage on ice is 0.1 monolayer independent of temperature.

Figure 3. The sensitivity of HNO_3 coverage on ice to the HCl vapor pressure as a function of temperature. All the lines except the lowest one are calculated by assuming adsorption energies of -14.2 kcal mol^{-1} for both gases. The lowest line is calculated by assuming adsorption energies of -14.2 and -16.2 kcal mol^{-1} for HNO_3 and HCl, respectively. The HNO_3 vapor pressure is set at 2 x 10^{-8} for all the calculations. The numbers on the lines indicate the HCl vapor pressure in units of torr times 10^8.

measurements [Weinheimer et al., 1998]. However lee wave clouds in general have short lifetimes, and therefore the HNO_3 removal process is almost entirely reversible. On the other hand, we believe irreversible removal of HNO_3 will only occur on cirrus in which the average ice crystal radii exceeds 100 micron (labeled in Figure 4 as precipitating cirrus). Ice crystals less than a 100 micron are unlikely to survive a 1.5 km (a typical cirrus cloud thickness [Dowling and Radke, 1990]) fall to below a cirrus cloud base [Rogers and Yau, 1989], where the majority of ice particles are evaporating. We refer to this class of clouds (average radii < 100 micron) as background cirrus (see Figure 4), and speculate that HNO_3 will be released back to the gas phase within a few kilometers from the altitude, where it was originally adsorbed. Since cirrus clouds often form between 1 to 3 km below tropopause [Dowling and Radke, 1990; Mace et al., 1997], it is unlikely that multiple background cirrus formation in this altitude band would result in removing HNO_3 to altitudes 3 km below the tropopause. Therefore, the adsorption process by background cirrus should also be to a large extent reversible.

For precipitating cirrus (streaks of ice particles often observed beyond the cirrus cloud base), less than 30% of gas phase HNO_3 may be irreversibly removed by cirrus per cloud

episode, depending on the cloud temperature and the ice number density. Although it is important to point out that the streaks of large ice particles are often observed in warm clouds (T > 230K) [e.g., *Sassen et al.*, 1989], and therefore the scavenging efficiency by precipitating cirrus is further reduced to below 10 % (see Figure 4) per cloud episode. For comparison in Figure 4 the fraction of HNO_3 removed by cirrus based on the assumption (a constant 0.1 monolayer coverage of HNO_3 on ice for all temperatures) used in the *Lawrence and Crutzen* [1998] study is also shown. It is clear that especially for a warm precipitating cirrus (T > 230 K), the assumption used by Lawrence and Crutzen will greatly overestimate the scavenging efficiency of HNO_3 by cirrus.

To fully assess the extent of HNO_3 removal by cirrus the scheme outlined here should be incorporated into a 3-D model, which is beyond the scope of this work. However by combining a few different types of datasets (aircraft and satellites) some qualitative information can be extracted on the effectiveness of cirrus to remove HNO_3. For instance, aircraft HNO_3 gas phase measurements in the upper troposphere over the Western Pacific (measurements taken during NASA PEM West A and B field programs) show a strong seasonal variation, with much higher concentrations measured during winter as compared to summer [*Thakur et al.*, 1999; *Tabazadeh et al.*, 1998]. Thus if cirrus was the main scavenger of HNO_3 in the upper troposphere, then one would expect noticeably more cirrus cloud cover over this location in the summer relative to winter in order to explain the seasonal trend observed in the HNO_3 data. On the contrary, SAGE II cirrus cloud statistics over the Western Pacific show only small seasonal variations in cirrus with roughly 15 % more cloud cover in winter as compared to summer [*Wang et al.*, 1996]. Obviously the weak seasonal trend in the cirrus cloud cover seen by SAGE II goes against the strong seasonal behavior observed in the HNO_3 data over the Western Pacific. Hence it is unlikely for cirrus to have been strongly involved in removing HNO_3 from the upper troposphere over this location. However, even though measurements over the Western Pacific (along with few other locations described in *Thakur et al.* [1999] showing the same seasonal trends in HNO_3) are suggestive in illustrating a lack of positive correlation between cirrus and HNO_3, they are not conclusive. In fact the seasonal variation seen in the HNO_3 data may be partly related to different sources of NO_y to the region during the two periods [*Thakur et al.*, 1999]. Thus future aircraft and satellite data combined with 3-D modeling studies are needed to better quantify the global relationship, which may or may not exist between cirrus and HNO_3.

Conclusions

In this paper we outlined a surface chemistry model for calculating HNO_3 coverage on ice in the upper troposphere. Current global chemistry-transport calculations indicate that assuming a constant surface coverage of about 0.1 monolayer of HNO_3 on ice could result in a significant depletion of gas phase HNO_3 by cirrus [*Lawrence and Crutzen, 1998*]. However we have shown that HNO_3 coverage on ice depends strongly on cirrus cloud temperature, HNO_3 vapor pressure and ice number density. Therefore assuming a constant surface coverage for all atmospheric conditions is not appropriate. The lack of a seasonal correlation between HNO_3 and cirrus over the Western Pacific may indicate that precipitating cirrus was not a key player in removing HNO_3 from the upper troposphere over this

location. Finally, to narrow down the range of uncertainty associated with the adsorption energy of HNO_3 on ice, which is the key parameter for surface chemistry calculations, laboratory data for HNO_3 adsorption on ice in the presence and absence of HCl and other possible competitive adsorbers at low vapor pressures and temperatures are needed.

References

Abbatt, J. P., K. D. Beyer, A. F. Fucaloro, J. R. McMahon, P. J. Wooldridge, R. Zhang, and M. J. Molina, Interaction of HCl vapor with water-ice: Implications for the stratosphere, *J. Geophys. Res.*, 97, 15,819, 1992.

Abbatt, J. P.D., Interaction of HNO_3 with water-ice surfaces at temperatures of the free troposphere, *Geophys. Res. Lett.*, 24, 1479, 1997.

Adamson, A. W., Physical Chemistry of Surfaces, John Wiley and Sons, Inc., 5th Ed., 1990.

Brasseur, G., and S. Solomon, Aeronomy of the Middle Atmosphere, Reidel Pub., 2nd Ed., 1986.

Dowling, D. R., and L. F. Radke, A summary of the physical properties of cirrus clouds, *J. Appl. Meteor.*, 29, 970, 1990.

Jacob, D., et al., Origin of ozone and NO_x in the tropical troposphere: A photochemical analysis of aircraft observations over the south Atlantic basin, *J. Geophys. Res.*, 101, 24,235, 1996.

Lacis, A. A., Radiative forcing of climate by changes in the vertical distribution of ozone, *J. Geophys. Res.*, 95, 9971, 1990.

Laidler, K. J., S. Glasstone, and H. Eyring, Application of the theory of absolute rates to heterogeneous processes, I. The adsorption and desorption of gases, *J. Chem. Phys.*, 8, 659, 1940.

Lawrence, M. G., and P. J. Crutzen, The impact of cloud particle gravitational settling on soluble trace gas distributions, *TELLUS, 50B*, 263, 1998.

Mace, G. G., T. P. Ackerman, E. E. Clothiaux, and B. A. Albrecht, A study of composite cirrus morphology using data from a 94-GHz radar and correlations with temperature and large-scale vertical motion, *J. Geophys. Res.*, 102, 13,581, 1997.

Rogers, R. R., and M. K. Yau, A short course in cloud physics, Pergamon Press, 3rd Ed., 1989.

Sassen, K., D. O., Starr, and T. Uttal, Mesoscale and microscale structure of cirrus clouds: Three case studies, *J. Atmos. Sci.*, 46, 371, 1989.

Singh H. B., et al., Reactive nitrogen and ozone over the western pacific: Distribution, Partitioning, and sources, *J. Geophys. Res.*, 101, 1793, 1996.

Tabazadeh, A., and R. P. Turco, A model for heterogeneous chemical processes on the surfaces of ice and nitric acid trihydrate particles, *J. Geophys. Res.*, 98, 12,727, 1993.

Tabazadeh A., et al., Nitric acid scavenging by mineral and biomass burning aerosols, *Geophys. Res. Lett.*, 25, 4185, 1998.

Thakur, A. N., H. B. Singh, P. Mariani, Y. Chen, Y. Wang, D. J. Jacob, G. Brasseur, J. F. Muller, and M. Lawrence, Distribution of reactive species in the remote free troposphere: Data and model comparisons, *Atmos. Env.*, 33, 1403, 1999.

Wang, P-H, P. Minnis, M. P. McCormick, G. S. Kent, and K. M. Skeens, A 6-year climatology of cloud occurrence frequency from stratospheric aerosols and gas experiment II observations (1985-1990), *J. Geophys. Res.*, 101, 29,407, 1996.

Weinheimer, A. J., T. L. Campos, J. G. Walega, F. E. grahek, B. A. Ridley, and E. J. Jensen, Uptake of NO_y on Wave-cloud ice particles, *Geophys. Res. Lett.*, 25, 1725, 1998.

Sommerfeld, R. A., C. A. Knight, and K. Larid, Diffusion of HNO_3 in Bulk Ice, *Geophys. Res. Lett.*, 25, 935, 1998.

Zondlo, M. A, Stephen B. Barone, and M. A. Tolbert., Uptake of HNO_3 on ice under upper tropospheric conditions, *Geophys. Res. Lett.*, 24, 1391, 1997.

A. Tabazadeh, NASA Ames Research Center, MS 245-4, Moffett Field, CA 94035-1000 (email:atabazadeh@mail.arc.nasa.gov).